Desalination and Water Treatment
www.deswater.com

doi: 10.1080/19443994.2012.749426

51 (2013) 4368–4378
June

Taylor & Francis
Taylor & Francis Group

Efficient removal of fluoride using new composite material of biopolymer alginate entrapped mixed metal oxide nanomaterials

S.K. Swain[a], Tanushree Patnaik[b], R.K. Dey[c,*]

[a]*Department of Applied Chemistry, Birla Institute of Technology, Mesra, Ranchi 835 215, India*
[b]*Department of Chemistry, Stewart Science College, Cuttack 753 008, India*
[c]*Centre for Applied Chemistry, Central University of Jharkhand, Ranchi 835 205, India*
Tel. +91 671 2306624; email: ratan.dey@cuj.ac.in

Received 29 September 2012; Accepted 9 November 2012

ABSTRACT

The present work reports preparation of a newly developed hybrid material of (Al/Ce)-alginate (Aluminium-Cerium-Calcium-Alginate [ACCA]) micro particles. The hybrid material was characterized by various instrument techniques. The average particle size of Al/Ce mixed metal oxide was found to vary between 29.39 to 553.2 nm. The XRD pattern of ACCA shows most significant peaks at 15.6, 28.4, 31.8, 45.3, 47.6, 56.5, 66.1, 75.3, and 83.9 in the 2θ range of 10–90°. The inorganic–organic hybrid material has the ability to remove fluoride from aqueous solution at the solid–liquid interface. The sorption of fluoride follows pseudo-second-order kinetics. Application of linearized form of Freundlich equation indicated the occupancy of 43.2% of active adsorption sites containing equal energy and a favorable condition for the adsorption of fluoride. The positive value of thermodynamic parameter (ΔS°) indicates increasing randomness during the sorption process. The influence of pH upon sorption–desorption characteristic of the hybrid material was quite prominent as evident from leaching of 89% of fluoride at pH 12. A possible mechanism of fluoride removal by the hybrid material was also proposed. Further, the reusable properties of the material support development for commercial application purpose.

Keywords: Alginate; Hybrid material; Nanocomposite; Fluoride; Adsorption; Kinetics

1. Introduction

Recent advancement in nanoscience and technology offers a wide range of solution to fabricate new materials for adsorption application [1]. Fluoride contamination in ground water is a worldwide problem, and hence, need to be addressed with utmost priority. Presence of excess quantity of fluoride in drinking water can give rise to a number of adverse effects [2]. The World Health Organization has set the maximum permissible concentration of fluoride in drinking water between 0.5 and 1.5 mg L^{-1} [3]. It is essential that an excess amount of fluoride in drinking water should be removed using appropriate material and technologies [4]. A number of review papers highlighted availability of various materials and methods, such as membrane filtration, electro-coagulation flotation, fluidized-bed precipitation, and ion exchange, that can be used for removing/reducing the concentration of fluoride in drinking water [5,6]. However, these methods being technically improved, requires trained man power and

*Corresponding author.

energy and involves cost factor. Adsorption is one of the simplest methods used successfully for defluoridation process with wide range of materials. Adsorption has additional advantages attributed to low cost, simple procedure, and sustainable method [7].

Use of biosorbents is gaining importance as an alternative for fluoride removal [8]. Tian et al. [9] demonstrated the ability of modified native cellulose fibers that can be useful for adsorption of both fluoride and arsenic. In this aspect, considerable work has been conducted in developing new adsorbents loaded with metal ions for the purpose of adsorptive removal of fluoride [10]. The metal ions adsorbed onto porous adsorbents or carrier materials have also shown promising results. For example, materials such as zirconium (Zr) (IV)-impregnated collagen fiber have also been studied for its defluoridation capacity [11]. Zr (IV) was found to be uniformly dispersed in collagen through chemical bond formation. Interestingly, for such of kind of material, the adsorption capacity increased with the rise in temperature. The kinetics of adsorption of fluoride onto Zr(IV)-impregnated collagen fiber could be described by Lagergren's pseudo-first-order rate model. Similarly, biosorbents such as alginate, chitin, and various chitosan derivatives have also attracted wide attention for their significant fluoride removal properties [5,12,13].

Alginate, in Fig. 1, is also projected as a suitable biopolymer that can be considered as adsorbent material after suitable chemical modification. Alginate is a polyuronide-type polysaccharide composed of different proportions of β-D-mannuronic acid and α-L guluronic acid units, linked by β-1–4 and α-1−4 bonds. The proportions and sequence distribution of these units along the polysaccharide chain vary according to the natural source. Alginates posses a very interesting ion-bonding feature that has attracted considerable attention and many studies focused on this property have been carried out. Further, alginate possesses unique functional properties, such as thickening and jellification. This functional properties are demonstrated when alginate is added into an aqueous solution in which swelling and thickening of the solution occurs with increasing solution viscosity. Solution viscosity and gel strength depend on temperature, pH, and presence of metal cations. Cross-linking of calcium alginate with glutaraldehyde was examined for its potential for fluoride removal capacity by batch equilibrium and column flow adsorption studies [14].

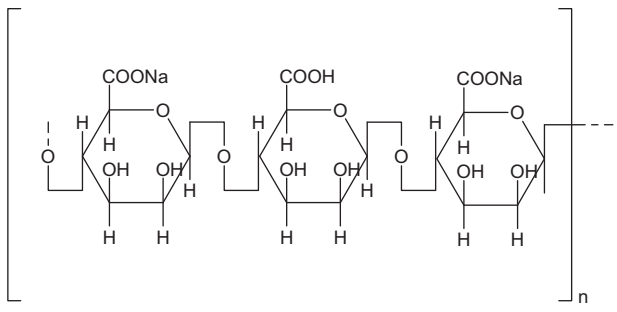

Fig. 1. Sodium alginate with mannuronate/guluronate residues.

It is known that metals like aluminium and cerium posses good fluoride complexation capacities. Use of mixed metal sorbents for defluoridation of drinking water has been attempted by researchers with various degree of success [15–17]. However, when such kind of materials is used in continuous column operation studies, there is a possibility of development of higher pressure drop. In order to overcome the difficulties, polymer entrapment of metal nanoparticles is a recently exploited field of research for the improvement or modification of material properties [18,19]. Keeping in view the interesting properties of alginate, the present investigation is aimed at preparation of alginate entrapped nanostructured Al(III)–Ce(IV) binary mixed oxide using a low-cost, eco-friendly procedure. Further, it is worth emphasizing that this procedure has the distinct advantages of simple preparation procedure and faster kinetics attributed to electrostatic interaction with the surface. The applicability of this material for defluoridation of drinking water is also reported.

2. Materials and methods

2.1. Chemicals

All chemicals used were of analytical grade (E. Merck, India). Double distilled water was used in all experiments. Stock solution of fluoride was prepared by dissolving 2.21 gm of sodium fluoride in one liter de-ionized water. The required concentration of fluoride solution was prepared by serial dilution of 1,000 mg L^{-1} fluoride solution.

2.2. Synthesis of Al–Ce mixed oxide nanoparticles

Al–Ce mixed oxide was prepared by mixing acidified $Al(NO_3)_3{\cdot}9H_2O$ (0.1 M) and $Ce(NO_3)_3{\cdot}6H_2O$ (0.1 M) solution in 1:1 volume ratios. The mixed solutions were stirred for 0.5 h at 60 °C. To the hot well-stirred mixed solutions, sodium hydroxide (1.0 M) was added slowly until the pH reaches 8.0 and stirring was continued for another 0.5 h. A white precipitation formed during mixing was allowed to remain in contact with mother liquor for 24 h, after which it was filtered and washed with de-ionized water until neutral pH. The solid residue was dried at 80 °C in an air oven.

2.3. Synthesis of Al–Ce loaded calcium alginate bead

A 2.0 g of sodium alginate powder was dispersed in 100 mL de-ionized water. This solution was mixed with a mechanical stirrer at 200 rpm keeping solution temperature at 60°C until a translucent, viscous solution was obtained. Then, 1.0 g of Al–Ce nanoparticle was mixed with the above viscous solution and allowed to stir for 2 h. Al–Ce loaded calcium alginate beads (Aluminium-Cerium-Calcium-Alginate [ACCA]) were obtained by dropwise addition of viscous solution (using a glass syringe) to 2% $CaCl_2$ solution with slow stirring. Thus, it was observed that beads of approximately 2.8–3.0 mm in diameter were formed which was allowed to keep in contact with $CaCl_2$ solution for further 24 h at 5°C. This process led to the formation of stable gel beads. Finally, all beads were washed several times with distilled water and dried in the vacuum drying chamber at (53 ± 2)°C for 24 h.

2.4. Adsorption

The adsorption studies for fluoride removal from drinking water by ACCA material were carried out in batch process. A 50 mL fluoride solution of desired concentration was taken into PVC conical flask and known weight of adsorbent was added into it and was shaken for 24 h on horizontal rotary shaker (shaking speed 200 rpm) to attain the equilibrium. Initial fluoride concentration was maintained at 10 mg L^{-1} for all the experiments except in those where the effects of initial fluoride concentration is to be studied. Adsorbent was then separated by filtration and the filtrate was analyzed for residual fluoride concentration using ion-selective electrode. All adsorption experiments were carried out at room temperature (25 ± 2)°C, except for the case where temperature variation is a parameter. The pH of the solution was adjusted using either HCl or NaOH. The effect of co-anions, such as chloride, sulfate, nitrate, bicarbonate, and phosphate upon the adsorption process, was studied by adding required amount of NaCl, Na_2SO_4, $NaNO_3$, $NaHCO_3$, and NaH_2PO_4 to a 100 mL of 10 mg L^{-1} fluoride solution.

The fluoride adsorption capacity was calculated using following equation:

$$q_e = (C_0 - C_e)(V/W) \times 100 \quad (1)$$

where q_e is the adsorption capacity (mg g^{-1}) in the solid at equilibrium; C_0 and C_e are initial and equilibrium concentrations of fluoride (mg L^{-1}), respectively; V is volume of the aqueous solution (L) and W is the mass (g) of adsorbent used in the experiments.

The reusability of adsorbent material was checked by adding 1.0 g of adsorbent to 50 mL of 10 mg L^{-1} fluoride solution. The adsorbent was filtered and dried in an oven at 70°C in vacuum. Subsequently, the same dried adsorbent material was used repeatedly for fluoride removal in various samples to determine the extent of adsorption. Further desorption studies were carried out by using the fluoride adsorbed adsorbents at different pH of the medium. Each experiment was carried out in duplicate and the average results were presented in the work.

2.5. Instrumentation

The FTIR spectra of sample materials were recorded at room temperature at a resolution of 4 cm^{-1} and 64 scans using Shimadzu IR Prestige-21 FTIR instrument. Scanning Electron Micrograph (SEM) of the sample was obtained in a JSM 6390 LV apparatus coupled with Energy Dispersive Spectroscopy (EDS). The particle size analysis of Al–Ce mixed oxide particle was carried out by Malvern Zetasizer Nano ZS by DLS method. The optical microscopic image was taken using Leica EZ 4D optical microscope. The X-ray diffraction pattern was obtained on a Shimadzu model XD3A diffractometer (40 kV/30 mA), in the range of $2\theta = 1.5$–70^o with a nickel-filtered CuKα radiation, at wavelength of 1.54 Å. Using Quantachrome automated gas sorption system, BET surface area measurement was done. The Thermogravimetric analysis (TGA/DTA) was carried out using Shimadzu DTG 60 in nitrogen atmosphere under a flow of 30 mL min^{-1} and heating rate of 10°C min^{-1} varying the temperature from 25–1,000°C. Concentration of fluoride in the solution, before and after adsorption, was determined using ion-selective electrode (Orion 720 A^+ Ion analyzer).

3. Results and discussion

3.1. Sorption studies

The nanoparticle-incorporated alginate matrix can be of interest for the removal of fluoride from water bodies. Hence, in order to obtain optimized results for the adsorption of fluoride by the hybrid material, a series of variation of parameters were studied under controlled conditions. At first, the effect of the adsorbent (ACCA) dose on the removal of fluoride was studied at an ambient temperature of (25 ± 2)°C with a contact time period of 5 h. The initial concentration of fluoride in the solution was maintained at 10 mg L^{-1}. It was observed that the percentage of the removal of fluoride increases with an increase in the adsorbent

dose. The observed result could be attributed to the availability of more sites of adsorption. Further, the percentage of the maximum removal of fluoride was found to be 97.2 with 20.0 g L^{-1} of ACCA.

It is known that solution pH is an important parameter that controls the adsorption at the water-adsorbent interfaces. In the present investigation, the fluoride adsorption properties were examined in pH range of 2.0–12.0 (Fig. 2). Fluoride adsorption was found to increase with an increase in pH of the medium. This may be attributed due to the strong competition of the hydroxyl ions with the fluoride ions in the solutions. In an acidic medium, the formation of weak hydrofluoric acid often influences the amount of fluoride adsorption by the adsorbent material. The percentage of the maximum removal of fluoride (97.2%) could be possible at pH 7.0.

Variation of contact time is another most important parameter to study the fluoride removal characteristics of the material. In present investigation, it was found that fluoride uptake increases with contact time period (Fig. 3) and the equilibrium saturation point was obtained in 180 min. It may be noted that initially, all adsorbent sites were available for the anion coordination and initial solute concentration gradient was also high. Once the saturation of metal sites was attained, the rate of fluoride uptake remained almost constant due to further decrease in the number of available adsorbent sites as well as the amount of the remaining fluoride ions in the solution.

To better understand the kinetics of adsorption process by the hybrid material, three different kinetic models were used to fit the experimental data: (i) the pseudo-first-order, (ii) the pseudo-second-order, and

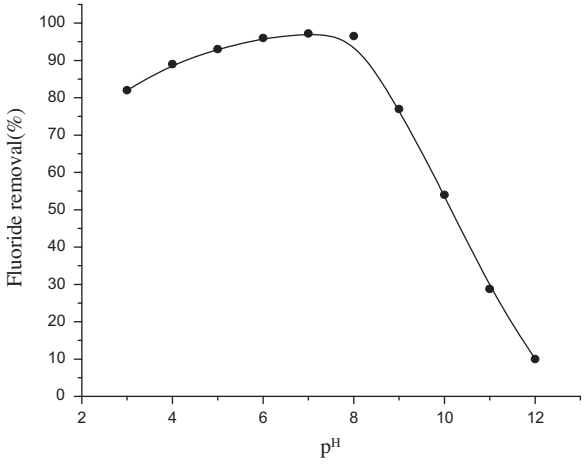

Fig. 2. Effect of pH on extent of removal of fluoride by ACCA, conc. of fluoride: 10 mg L^{-1}; time of contact: 300 min; and adsorbent dose: 20.0 g L^{-1}.

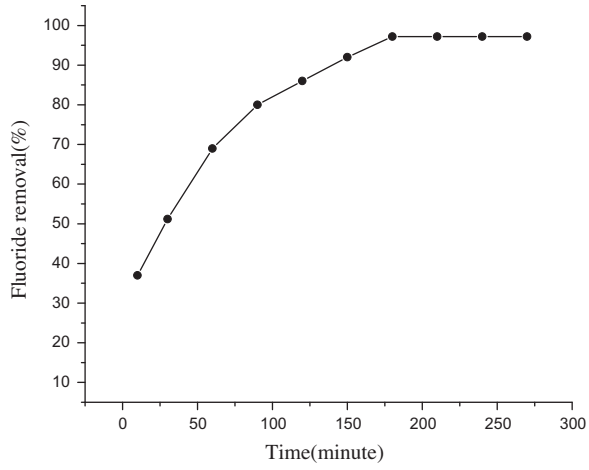

Fig. 3. Effect of contact time on fluoride adsorption by ACCA, conc. of fluoride: 10 mg L^{-1}; adsorbent dose: 20 g L^{-1}; and pH: 7.0.

(iii) the intra-particle diffusion model [4]. The pseudo-first-order model was developed for irreversible sorption of solid/liquid systems which is described by the following rate equation:

$$\mathrm{In}(q_e - q_t) = \mathrm{In}q_e - K_f t \quad (2)$$

where q_e and q_t denote the amount of fluoride adsorbed (mg g^{-1}) at equilibrium and at time "t", respectively. K_f (min^{-1}) is the rate constant of pseudo-first-order reaction. By plotting $\ln(q_e - q_t)$ vs. t, a straight-line relationship should be obtained. Values of both q_e and K_f can be determined from the intercept and slope of the curve, respectively.

The pseudo-second-order model is based on the assumption that chemical sorption or chemisorption is one of the factors controlling the sorption kinetics [3,25]. The rate expression can be written as:

$$t/q_t = 1/K_s(q_e)^2 + t/q_e \quad (3)$$

where K_s is the rate constant for pseudo-second-order reaction (g mg^{-1} min^{-1}). q_e and q_t are the amounts of solute sorbed at equilibrium and at any time "t" (mg g^{-1}), respectively. The straight-line plot of t/q_t vs. t for the kinetic data gives the values for q_e and K_s, respectively, from the slope and intercept.

The intra-particle diffusion model [25] can be expressed as:

$$q_t = K_i t^{1/2} + C \quad (4)$$

where K_i is the intra-particle diffusion constant (mg g^{-1} $min^{-1/2}$) and C is intercept. The value of K_i is

determined from the slope of the plot q_t vs. $t^{1/2}$. The value of intercept C provides information about the thickness of boundary layer i.e. the resistant to external mass transfer.

The sorption kinetic was studied at temperature: (25 ± 2)°C; initial fluoride concentration: 10 mg L^{-1}; adsorbent dose: 20.0 g L^{-1}; and pH: 7.0. Values of different kinetic parameters, presented in Table 1, were obtained from various graphical presentations of kinetic equations. In intra-particle diffusion model (Weber-Morris plot), the value of intercept C provides information about thickness of boundary layer, i.e. the resistance to external mass transfer [26]. The deviation of straight line from the origin may be due to the difference between the rate of mass transfer in the initial and final stages of adsorption, which indicates that the pore diffusion may not be the sole controlling step.

Hence, as shown in Table 1, the value of correlation coefficient (R^2) for the pseudo-second-order kinetic model was found to be 0.996. In addition, the values of $q_{e,exp}$ and $q_{e,cal}$ were also found close to each other. The result indicated that the sorption process could be expected to follow a pseudo-second-order kinetics.

Increase in initial fluoride concentration shows reduction in fluoride uptake by the hybrid material which mainly is attributed to the saturation of available coordination sites. In this regard, evaluation of isotherm models is one of the basic requirements for successful design of any commercial adsorption system. Therefore, in the present investigation, experimental equilibrium data were fitted to four different adsorption isotherms i.e. Langmuir, Freundlich, Temkin, and Dubinin—Radushkevich (D–R) [26,27]. Quantitative evaluation of the Langmuir adsorption model was done using following empirical equation [28]:

$$1/q_e = (1/K_L q_m)(1/C_e) + 1/q_m \quad (5)$$

where q_e is the amount of fluoride adsorbed at equilibrium (mg g^{-1}), C_e is the equilibrium concentration (mg L^{-1}), q_m is the mono-layer adsorption capacity (mg g^{-1}), and K_L is the Langmuir constant related to the free adsorption energies (L mg^{-1}). The value of q_m and K_L can be calculated, respectively, from the slope and intercept of the linear plot of $1/C_e$ vs. $1/q_e$. The adsorption efficiency is evaluated by dimensionless equilibrium parameter (R_L) by using following equation:

$$R_L = \frac{1}{1 + K_L C_0} \quad (6)$$

and the value $R_L < 1$ indicates a favorable adsorption process.

It is to be mentioned that Freundlich isotherm model assumes that the concentration of adsorbent on the adsorbate surface increases with the adsorbent concentration [29,30]. Hence, Freundlich equation is widely applicable to various heterogeneous systems and it is characterized by a heterogeneity factor $1/n$. The linearized form of Freundlich equation can be represented as:

$$\text{In } q_e = \text{In } K_f + 1/n \text{ In } C_e \quad (7)$$

Application of Temkin isotherm model is based on the adsorbent–adsorbate interactions which are linear in nature and the adsorption is characterized by uniform distribution of binding energies. The linearized form of Temkin isotherm can be represented as:

$$q_e = B_1 \text{ In } A + B_1 \text{ In } C_e \quad (8)$$

where A is the equilibrium binding constant (L mol^{-1}) corresponding to the maximum binding energy and the constant B_1 is related to the heat of adsorption. A plot of q_e vs. ln C_e enables the constant B_1 and A to be determined from the slope and intercept, respectively.

The linearized form of D–R isotherm is represented as:

$$\text{In } q_e = \text{In } q_m - K\varepsilon^2 \quad (9)$$

where ε^2 is the Polanyi potential which is equal to RT ln $(1 + 1/C_e)$. q_e is the amount of adsorbate adsorbed at equilibrium per unit of adsorbent (g g^{-1}), q_m is the

Table 1
Kinetic parameters for fluoride adsorption onto ACCA

Pseudo-first-order[a]				Pseudo-second-order[a]				Intra-particle diffusion[a]		
q_{exp}	K_f	$q_{e,cal}$	R^2	K_s	h	$q_{e,cal}$	R^2	K_i	C	R^2
0.486	0.016	0.3819	0.990	0.063	0.0187	0.545	0.996	0.029	0.1	0.988

[a]The units for q_{exp}, $q_{e,cal}$: mg g^{-1}; K_f: L min^{-1}; K_s, h: (mg g^{-1} min^{-1}); K_i, C: mg (g $min^{1/2})^{-1}$.

theoretical saturation capacity ($g\,g^{-1}$), and C_e is the equilibrium solid concentration ($g\,L^{-1}$). K is the constant related to adsorption energy. R is the gas constant and T is the temperature in Kelvin. The value of K and q_m, respectively, is obtained from the slope and intercept of the plot of q_e vs. ε^2.

The linear fitting presentations for all isotherm models are presented in Fig. 4, and corresponding values are presented in Table 2. The linearized form of Freundlich equation ($1/n = 0.432$ by linear method) indicate that nearly 43.2% of active adsorption sites contain equal energy for adsorption process. Similarly, the value of R_L (for an initial fluoride concentration of $10\,mg\,L^{-1}$) was found to be 0.0522 and 0.197 obtained by liner and nonlinear regression analysis, respectively, indicating a favorable condition for the adsorption of fluoride. Value of heat of adsorption (B_1), evaluated using Temkin model, was $0.329\,kJ\,mol^{-1}$. Linearized form of D–R model estimated the values of adsorption energy (E) as $10\,kJ\,mol^{-1}$, suggesting that the adsorption proceeded by an ion-exchange process [27].

Thus, in order to evaluate the best fitting of isotherm equations to experimental data, various error functions, such as: the sum of square of errors (SSE), the sum of absolute errors (SAE), the average relative errors (ARE), the hybrid fractional errors (HYBRID), the Marquardt's percent standard deviation (MPSD), and relative standard deviation (R^2), were examined [28]. The computational result of all six different error functions using linear approach is presented in Table 3. It was found that the Freundlich isotherm model was the most suitable model to describe the adsorption phenomenon in present investigation. The evaluation was based on the obtaining highest R^2 value and lowest SSE, SAE, ARE, HYBRID, and MPSD values from the computational result.

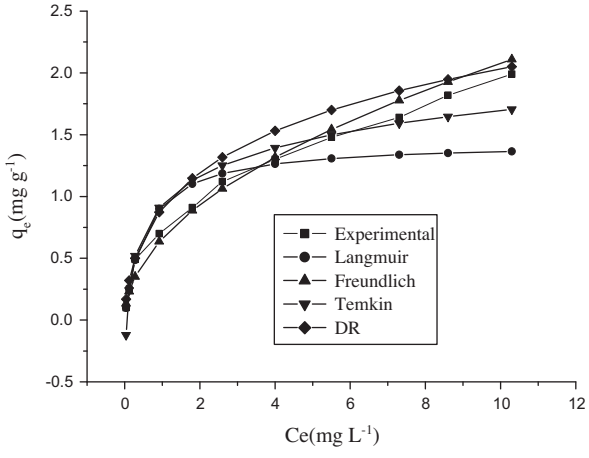

Fig. 4. Adsorption isotherm modeling of fluoride removal using ACCA using linear regression analysis; adsorbent dose: $20.0\,g\,L^{-1}$; pH, 7.0, Temp, (25 ± 2)°C; and contact time: 210 min.

Table 2
Linear Freundlich, Langmuir, Temkin, and D–R isotherm constants related to the sorption of fluoride onto ACCA

Model/parameters	Linear method
Freundlich	
K_F	0.6616
$1/n$	0.497
Langmuir	
K_L	1.8158
qm	1.438
Temkin	
b	7,530.61
A	17.306
D–R	
q_m	0.00391
K	0.005

It is known that adsorption process is influenced by the temperature of the medium. Hence, the effect of temperature on adsorption was also studied in a range of 10–50°C. The result of the investigation showed that the amount of adsorption of fluoride increases with increase in temperature of the medium. Hence, the feasibility of adsorption process was further computed using thermodynamic relationship i.e. by applying Van't Hoff's equation [29,30] which is represented as:

$$\Delta G^\circ = -RT \ln K_d \tag{10}$$

where R is the universal gas constant ($8.314\,J\,mol^{-1}\,K^{-1}$), T is the temperature (K), and ΔG° is the change in free energy. Further, the relationship between distribution coefficient (K_d), enthalpy (ΔH°), and entropy (ΔS°) was evaluated by using following thermodynamic equation:

$$\ln K_d = \Delta S^\circ/R - \Delta H^\circ/RT \tag{11}$$

Both ΔH° and ΔS° were calculated, respectively, from the slope and intercept of plot of ln K_d vs. $1/T$. The values of all thermodynamic parameters are presented in Table 4 which show the spontaneity of the adsorption process as evident from the negative values of ΔG° at all temperature. Further, positive value of ΔS° indicates the increasing randomness during the

Table 3
Isotherm error deviation data related to the sorption of fluoride on to ACCA six commonly used functions

Error functions	R^2	SSE	SAE	ARE	HYBRID	MPSD
Linear approach						
Freundich	**0.997**	**0.008**	**0.792**	**19.563**	**12.646**	**22.993**
Lanmuir	0.996	0.801	2.058	21.761	16.714	23.141
Temkin	0.931	0.278	1.430	57.874	36.933	107.226
D–R	0.990	0.308	1.635	41.271	25.587	43.279

Table 4
Thermodynamic parameters for the sorption of fluoride on ACCA

Temp (°C)	ΔH° (kJ mol^{-1})	ΔS° (kJ mol^{-1} K^{-1})	ΔG° (kJ mol^{-1})	Ea (kJ mol^{-1})	S^*
10	47.647	0.219	−14.51	45.88	0
20			−16.71		
30			−18.90		
40			−21.11		
50			−23.30		

sorption process and positive value of ΔH° confirms the endothermic nature of adsorption.

In this regard, computation of sticking probability (S^*) is quite helpful in relating surface coverage (θ) of the adsorbent by the adsorbed molecules and the activation energy associated with the process [31]. Hence, the relationship can be given by:

$$S^* = (1-\theta)\exp(-E_a/RT) \quad (12)$$

$$\text{where } \theta = 1 - C_e/C_0 \quad (13)$$

Both the value of E_a and θ can be calculated, respectively, from the slope and intercept of the plot of $\ln(1-\theta)$ vs. $1/T$. In present investigation, the value of sticking probability was found to be 0 which indicates that the adsorption follows a chemisorption process [27,31].

Drinking water may contain several other ions, such as sulfate, chloride, nitrate, etc., along with fluoride, which may compete with fluoride for active sorption sites. Therefore, the effect of various diverse ions/competing co-ions upon adsorption of fluoride was also investigated using the experimental condition for initial fluoride concentration at 10 mg L^{-1}, while varying the initial concentration of co-ions (sulfate, nitrate, bicarbonate, and phosphates) from 0 to 600 mg L^{-1}. The result of the observation for the effect of co-ions indicated that NO_3^-, Cl^{-1}, and SO_4^{2-} had little effect upon fluoride removal processes. However, the experimental result also showed that the presence of PO_4^{3-} and HCO_3^{-1} do significantly affect the fluoride removal process. Thus, presence of PO_4^{3-} and HCO_3^{-1} reduces uptake of fluoride to 56 and 52%, respectively. Similar kind of result was also reported earlier by various other researchers [27]. Although such kind of problem is not unusual, other treatment processes can also be adopted to remove such interfering ions prior to the removal of fluoride using adsorbent. The reusable properties of ACCA, evaluated using dried adsorbent material, showed reduction of material efficiency from 97.2 to 60% following a sequence of first to seventh cycle of batch operation study. On the other hand, the result of desorption study indicated negligible leaching of fluoride in acidic pH (Fig. 5).

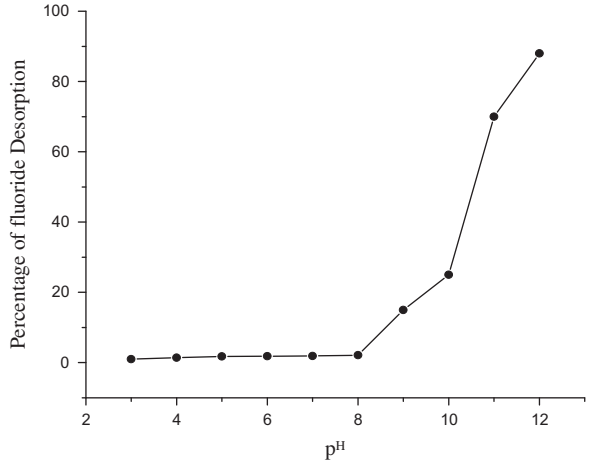

Fig. 5. Desorption of fluoride from ACCA with variation of pH of the medium.

Alkaline pH (pH > 8) strongly favors elution where nearly 88% of the fluoride could successfully be leached out from the adsorbent material at pH 12.0.

In order to give insight into the mechanistic aspect of defluoridation capacity of the material, it is proposed that calcium alginate form aqua complex with water and develops surface charge through amphoteric dissociation process [31]. At acidic pH of the medium, positively charged surface sites are developed which attract the negatively charged fluoride ions by electrostatic attraction resulting in the enhanced fluoride removal at acidic pH. This can be presented by following equations:

$$MOH + H^+ \rightarrow MOH_2^+ \quad (14)$$

$$MOH_2^+ + F^- \rightarrow MF + H_2O \quad (15)$$

$$\text{Overall reaction : } MOH + H^+ + F^- \rightarrow MF + H_2O \quad (16)$$

where M = metal ions like Al^{3+} and Ce^{4+}.

At neutral pH of the solution, fluoride adsorption can be due to the ligand-exchange reaction between fluoride and hydroxyl ions.

$$M - OH + F^- \rightarrow M - F + OH^- \quad (17)$$

The exchange mechanism between fluoride and hydroxide ion was further conformed by observation of decrease in pH of the solution after treatment with the adsorbent. Thus, decrease in adsorption at higher pH of the medium may be due to the abundance of hydroxyl ions which leads to increased hindrance to diffusion of fluoride ion.

3.2. Characterization

Material characterization is one of the most important studies to establish the identity and physical/chemical properties of the material. Hence, the hybrid material was characterized by using various instrumentation techniques. The size distribution of Al–Ce mixed oxide is presented in Fig. 6. The particle size of the Al–Ce mixed oxide was found to be in the range of 29.39–553.2 nm. The optical microscope picture of calcium alginate entrapped Al/Ce mixed oxide is also shown in Fig. 7. The average diameter of Al–Ce-entrapped calcium alginate was found to be 3.14 nm. The surface area, micro pore volume, and average micro pore diameter of ACCA were determined to be 89.23 m^2g^{-1}, 0.202 cm^2/gm, and 46.32 Å, respectively.

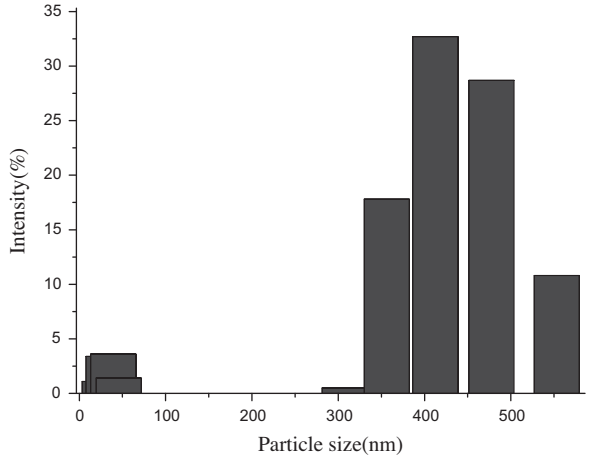

Fig. 6. Size distribution plot of Al–Ce mixed oxide.

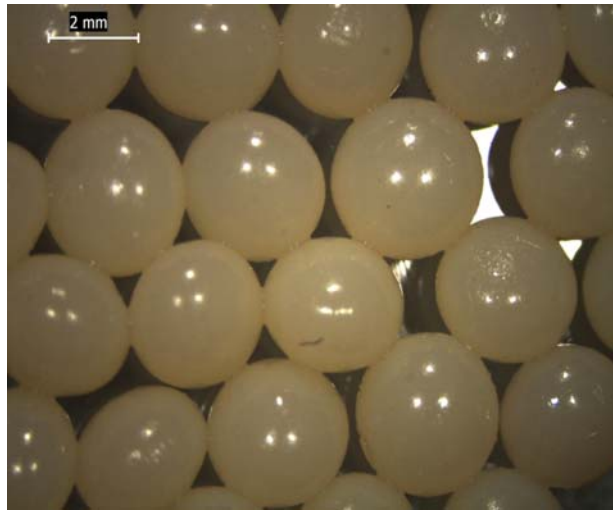

Fig. 7. Optical microscope image of ACCA.

The EDS spectrum embedded SEM of the fluoride-adsorbed ACCA is furnished in Fig. 8. The micrographs show the presence of F in addition to presence of Al and Ce. The EDS mapping of ACCA is also furnished in Fig. 9. The mapping confirmed the presence of Al (shown in shown in red color) and Ce (shown in blue color) that are evenly distributed upon material surface.

The XRD pattern of the hybrid material, obtained in the range of $2\theta = 10–90^\circ$, is illustrated in Fig. 10. The most significant peaks are noted at 15.6, 28.4, 31.8, 45.3, 47.6, 56.5, 66.1, 75.3, and 83.9. The result indicated that the hybrid material is crystalline in nature containing oxides of Al and Ce [32,33]. Thus, XRD study also provides an alternative evidence of presence of metal particles in the alginate matrix.

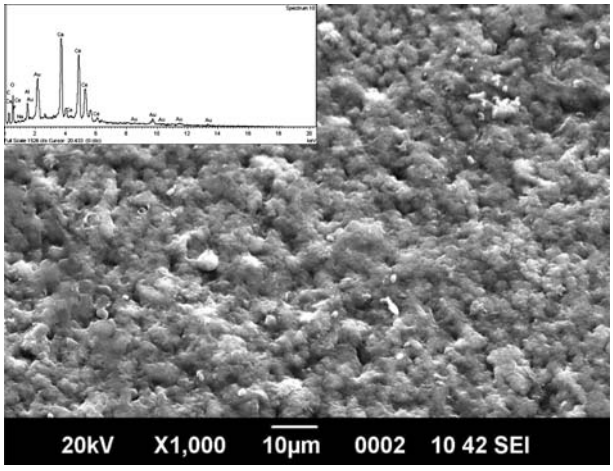

Fig. 8. The SEM embedded with EDS showing the surface morphology of fluoride adsorbed ACCA.

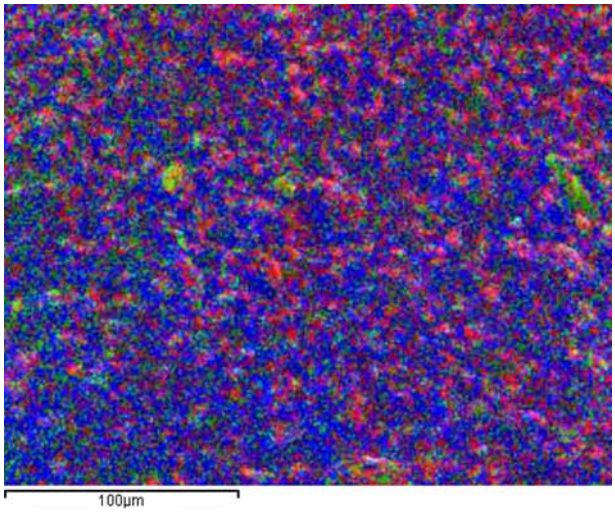

Fig. 9. The EDS Mapping of ACCA (yellow, carbon; green, calcium; blue, cerium; grey, oxygen; and red, aluminum).

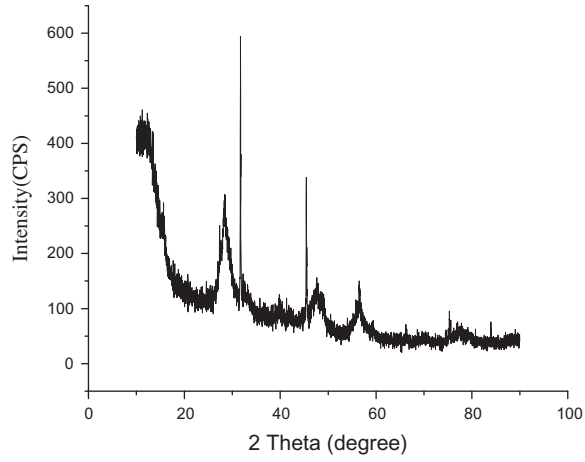

Fig. 10. X-ray diffraction pattern of ACCA showing the crystalline nature of hybrid material.

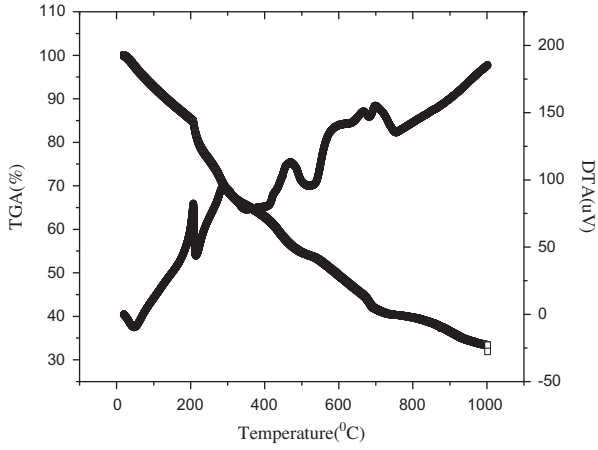

Fig. 11. Thermal analysis showing TGA and DTA of adsorbent (ACCA).

Thermogravimetric analysis is an important characterization technique for evaluating the behavior of material with respect to temperature parameter [34,35]. The TGA-DTA curves for the ACCA in the range 25–1,000°C is shown in Fig. 11. The graph shows more or less a gradual weight loss pattern in the range of study. It is understood that the metal particles might be bound with some surface functional groups of alginate, thus making them less hydrophilic in nature. The weight loss observed between 25–205°C could be attributed to the evaporation of bonded water/surface hydroxyl groups/solvent present in the alginate matrix. The corresponding DTA shows endotherm peak in the range 25–205°C (weight loss 14.7%). The weight loss in the range 205–310°C is attributed to desorption and preliminary degradation of alginate (weight loss 17%). The weight loss observed in the range 310–480°C (weight loss 12.1%) and 480–700°C (14%) could be due to the further degradation of alginate. For all above TGA observation, corresponding DTA shows endothermic peak thus supplementing the evidence. The total weight loss occurred within the range of study is about 66.25%. The metallic residue remaining at 1,000°C is about 33.75% attributed mainly to the presence of various oxide materials.

The FTIR spectra of alginate, ACCA, and fluoride-adsorbed ACCA are furnished in Fig. 12. The broad peak around 3,253 cm^{-1} shows the presence of bonded hydroxyl group. The absorption peak at 1,604 cm^{-1} shows the stretching vibration of carbonyl group of carboxylic acid group. The peak at 1,080 cm^{-1} was

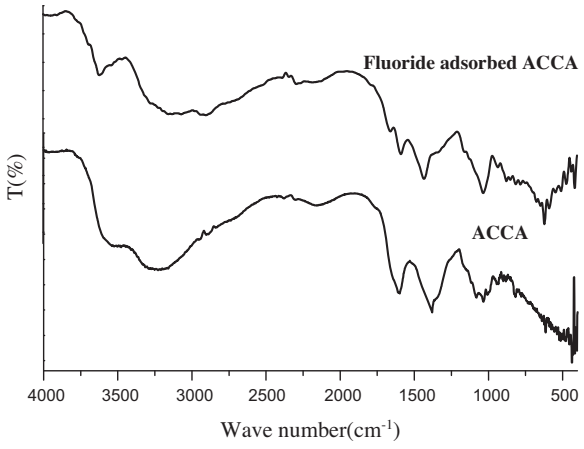

Fig. 12. The FTIR spectra of ACCA and fluoride adsorbed ACCA.

assigned to the C–O_{str} of –C–O–C– group. The spectrum of ACCA shows O–H_{str} vibration peak at 3,253 cm^{-1} shifted to 3,128 cm^{-1} in case of fluoride-adsorbed material. The disappearance of the peak present at 1,116 cm^{-1} is due to the fluoride adsorption on hydroxyl sites. Because –OH and F^- have nearly same size, they can exchange for each other and F^- can be suitably adsorbed [36,31]. Similarly, the asymmetric C–O_{str} frequency of ACCA is observed at 1,604 cm^{-1}. Peak observed between 1,200–400 cm^{-1} is assigned to characteristics of mixed metals. In case of fluoride-adsorbed material, peak appeared at 1,430 cm^{-1} is assigned to formation of Al–F bonds.

It is to be noted that the adsorption capacity q_m (mg g^{-1}) for ACCA was found to be 1.438. A comparative assessment of ACCA vis-à-vis other available commercial adsorbent was also done [1,3,6,7,15,31,37]. Materials such as Laterite [37] show a q_m (mg g^{-1}) value of 0.85. Similarly, some other materials such as Fe_3O_4 nanoparticle in a matrix [1] and many other materials [3] also show comparable efficiency. While solution parameters and many other factors, such as co-ions, etc, plays a vital role in evaluating the material efficiency, ACCA has the distinct advantage of separation of fluoride from drinking water at natural pH of the medium and further advantage of regeneration and reuse. Hence, ACCA provides a good option for further commercial exploitation that can be used in sustainable manner for fabrication of defluoridation kit for rural use.

4. Conclusions

The material prepared by the incorporation of Al–Ce mixed oxide nanoparticles in alginate polymeric material demonstrate a new kind of inorganic–organic hybrid material with improved efficiency. The material could be able to remove nearly 98% of fluoride at natural pH of water bodies (pH = 7.0) under given experimental condition. Adsorption process followed pseudo-second-order kinetics, further verified by using different adsorption isotherm models, that also shows applicability of Freundlich equation. Energy of adsorption (E), evaluated by DR model, was found to be 10 $mol^2\,kJ^{-2}$ suggesting an ion-exchange mechanism for the removal of fluoride. Evaluation of thermodynamic parameters shows negative value for Gibb's free energy (ΔG°) and positive value for ΔS°, respectively, indicating spontaneity and increasing randomness in adsorption process. The efficiency is further demonstrated by little effect of co-ions in the medium and successful adsorption–desorption in continuous cycles of operation, thus enhancing its possibility of future commercial application of the hybrid material.

Acknowledgements

Central Instrumentation Facility, BIT, Mesra; DST, New Delhi; and UGC, New Delhi.

References

[1] M. Bhaumik, T.Y. Leswifi, A. Maity, V.V. Srinivasu, M.S. Onyango, Removal of fluoride from aqueous solution by polypyrrole/Fe_3O_4 magnetic nanocomposite, J. Hazard. Mater. 186 (2011) 150–159.
[2] V. Hernández-Montoya, L.A. Ramírez-Montoya, A. Bonilla-Petriciolet, M.A. Montes-Morán, Optimizing the removal of fluoride from water using new carbons obtained by modification of nut shell with a calcium solution from egg shell, Biochem. Engg. J. 62 (2012) 1–7.
[3] Q. Guo, J. Eric, Reardon fluoride removal from water by meixnerite and its calcination product, Appl. Clay Sci. 56 (2012) 7–15.
[4] G. Zhang, Z. He, W. Xu, A low-cost and high efficient zirconium-modified-Na-attapulgite adsorbent for fluoride removal from aqueous solutions, Chem. Engg. J. 183 (2012) 315–324.
[5] P. Miretzky, A.F. Cirelli, Fluoride removal from water by chitosan derivatives and composites: A review, J. Fluorine Chem. 132 (2011) 231–240.
[6] M. Mohapatra, S. Anand, B.K. Mishra, D.E. Giles, P. Singh, Review of fluoride removal from drinking water, J. Environ. Management 91 (2009) 67–77.
[7] M. Mohapatra, D. Hariprasad, L. Mohapatra, S. Anand, B.K. Mishra, Mg-doped nanoferrihydrite—A new adsorbent for fluoride removal from aqueous solutions, Appl. Surf. Sci. 258 (2012) 4228–4236.
[8] A. Bhatnagar, E. Kumar, M. Sillanpää, Fluoride removal from water by adsorption—A review, Chem. Engg. J. 171 (2011) 811–840.
[9] Y. Tian, M. Wu, R. Liu, D. Wang, X. Lin, W. Liu, L. Ma, Y. Li, Y. Huang, Modified native cellulose fibers—A novel efficient adsorbent for both fluoride and arsenic, J. Hazard. Mater. 185 (2011) 93–100.
[10] Y.M. Zhou, C.X. Yu, Y. Shan, Adsorption of fluoride from aqueous solution on La^{3+}-impregnated cross-linked gelatin, Sep. Purif. Technol. 36 (2004) 89–94.

[11] X.P. Liao, B. Ishi, Adsorption of fluoride on zirconium(IV)-impregnated collagen fiber, Environ. Sci. Technol. 39 (2005) 4628–4632.
[12] J.L. Davila-Rodriguez, V.A. Escobar-Barrios, K. Shirai, J.R. Rangel-Mendez, Synthesis of a chitin-based biocomposite for water treatment: Optimization for fluoride removal, J. Fluorine Chem. 130 (2009) 718–726.
[13] D. Thakre, S. Jagtap, N. Sakhare, N. Labhsetwar, S. Meshram, S. Rayalu, Chitosan based mesoporous Ti–Al binary metal oxide supported beads for defluoridation of water, Chem. Eng. J. 158 (2010) 315–324.
[14] Y. Vijaya, S.R. Popuri, A.S. Reddy, A. Krishnaiah, Synthesis and characterization of glutaraldehyde-crosslinked calcium alginate for fluoride removal from aqueous solutions, J. Appl. Polym. Sci. 120 (2011) 3443–3452.
[15] H. Liu, S. Deng, Z. Li, G. Yu, J. Huang, Preparation of Al–Ce hybrid adsorbent and its application for defluoridation of drinking water, J. Hazard. Mater. 179 (2010) 424–430.
[16] B. Zhao, Y. Zhang, X. Dou, X. Wu, M. Yang, Granulation of Fe–Al–Ce trimetal hydroxide as a fluoride adsorbent using the extrusion method, Chem. Engg. J. 185–186 (2012) 211–218.
[17] L. Chen, B.Y. He, S. He, T.J. Wang, C.L. Su, Y. Jin, Fe-Ti oxide nano-adsorbent synthesized by co-precipitation for fluoride removal from drinking water and its adsorption mechanism, Powder Technol. 227 (2012) 3–8, doi:10.1016/j.powtec.2011.11.030.
[18] J. Kim, B.V. der Bruggen, The use of nanoparticles in polymeric and ceramic membrane structures: Review of the manufacturing procedures and performance improvement for water treatment, Env. Pollut. 158 (2010) 2335–2349.
[19] V. Kumar, N. Talreja, D. Deva, N. Sankararamakrishnan, A. Sharma, N. Verma, Development of bi-metal doped micro- and nano multi-functional polymeric adsorbents for the removal of fluoride and arsenic(V) from wastewater, Desalination 282 (2011) 27–38.
[20] I. Langmuir, The constitution and fundamental properties of solids and liquids, J. Amer. Chem. Soc. 38 (1916) 2221–2295.
[21] H. Freundlich, Über die adsorption in lösungen [On the adsorption in solution], Z. Phys. Chem. 57 (1906) 385–470.
[22] S. Figaro, J.P. Avril, F. Brouers, A. Ouensanga, S. Gaspard, Adsorption studies of molasses's wastewaters on activated carbon: Modelling with a new fractal kinetic equation and evaluation of kinetic models, J. Hazard. Mater. 161 (2009) 649–656.
[23] M. Malakootian, A. Fatehizadeh, N. Yousefi, M. Ahmadian, M. Moosazadeh, Fluoride removal using regenerated spent bleaching earth (RSBE) from groundwater: Case study on Kuhbonan water, Desalination 277 (2011) 244–249.
[24] E. Kumar, A. Bhatnagar, M. Ji, W. Jung, S.H. Lee, S.J. Kim, G. Lee, H. Song, J.Y. Choi, J.S. Yang, B.H. Jeon, Defluoridation from aqueous solutions by granular ferric hydroxide (GFH), Water Res. 43 (2009) 490–498.
[25] V. Sivasankar, T. Ramachandramoorthy, A. Darchen, Manganese oxide improves the efficiency of earthware in fluoride removal from drinking water, Desalination 272 (2011) 179–186.
[26] M. Mourabet, H. El Boujaady, A. El Rhilassi, H. Ramdane, M. Bennani-Ziatni, R. El Hamri, A. Taitai, Defluoridation of water using Brushite: Equilibrium, kinetic and thermodynamic studies, Desalination 278 (2011) 1–9.
[27] S.K. Swain, T. Patnaik, V.K. Singh, U. Jha, R.K. Patel, R.K. Dey, Kinetics, equilibrium and thermodynamic aspects of removal of fluoride from drinking water using meso-structured zirconium phosphate, Chem. Engg. J. 171 (2011) 1218–1226.
[28] S.J. Allen, Q. Gan, R. Matthews, P.A. Johnson, Comparison of optimized isotherm models for basic dye adsorption by kudzu, Biores. Technol. 88 (2003) 143–152.
[29] R.K. Dey, T. Patnaik, V.K. Singh, S.K. Swain, M.A. Melo, Jr., C. Airoldi, Al-centered functionalized inorganic–organic hybrid sorbent containing N and S donor atoms for effective removal of cadmium, Solid State Sci. 12 (2010) 440–447.
[30] D. Sumen, G. Sawati, C.G. Uday, Hydrous ferric oxide(HFO) a scavenger for fluoride from contaminated water, Water Air Soil Pollut. 158 (2004) 311–323.
[31] H. Lu, S. Deng, Z. Li, G. Yu, J. Huang, Preparation of Al–Ce hybrid adsorbent and its application for defluoridation of drinking water, J. Hazard. Mater. 179 (2010) 424–430.
[32] K. Biswas, D. Bandhoyapadhyay, U.C. Ghosh, Adsorption kinetics of fluoride on iron(III) zirconium(IV) hybrid oxide, Adsorption 13 (2007) 83–94.
[33] S.F. Lim, Y.M. Zheng, Uptake of arsenate by an alginate-encapsulated magnetic sorbent: process performance and characterization of adsorption chemistry, J. Colloid Interface Sci. 333 (2009) 33–39.
[34] M. Mohapatra, D. Hariprasad, L. Mohapatra, S. Anand, B.K. Mishra, Mg-doped nanoferrihydrite—Anewadsorbentforfluorideremovalfrom aqueous solutions, Appl. Surf. Sci. 258 (2012) 4228–4236.
[35] L.M. Nevárez, L.B. Casarrubias, O.S. Canto, A. Celzard, V. Fierro, R.I. Gómez, G.G. Sánchez, Biopolymers-based nanocomposites: Membranes from propionated lignin and cellulose for water purification, Carbohydrate Polym. 86 (2011) 732–741.
[36] H.X. Wu, T.J. Wang, L. Chen, Y. Jin, The role of the surface charge and hydroxyl group on a Fe–Al–Ce adsorbent in fluoride adsorption, Ind. Eng. Chem. Res. 48 (2009) 4530–4534.
[37] M. Sarkar, A. Banerjee, P.P. Parmanik, A.R. Sarkar, Use of laterite for the removal of fluoride from contaminated drinking water, Colloid. Interface Sci. 302 (2006) 432–444.